Journal of ELECTRONIC MATERIALS
DOI: 10.1007/s11664-016-4432-6

Ti/Pd/Ag Contacts to *n*-Type GaAs for High Current Density Devices

PENGYUN HUO [1,2] and IGNACIO REY-STOLLE[1,3]

1.—Instituto de Energía Solar – Universidad Politécnica de Madrid, ETSI de Telecomunicación, Avda. Complutense 30, 28040 Madrid, Spain. 2.—e-mail: huo.pengyun@ies-def.upm.es. 3.—e-mail: ignacio.reystolle@upm.es

The metallization stack Ti/Pd/Ag on *n*-type Si has been readily used in solar cells due to its low metal/semiconductor specific contact resistance, very high sheet conductance, bondability, long-term durability, and cost-effectiveness. In this study, the use of Ti/Pd/Ag metallization on *n*-type GaAs is examined, targeting electronic devices that need to handle high current densities and with grid-like contacts with limited surface coverage (i.e., solar cells, lasers, or light emitting diodes). Ti/Pd/Ag (50 nm/50 nm/1000 nm) metal layers were deposited on *n*-type GaAs by electron beam evaporation and the contact quality was assessed for different doping levels (from 1.3×10^{18} cm^{-3} to 1.6×10^{19} cm^{-3}) and annealing temperatures (from 300°C to 750°C). The metal/semiconductor specific contact resistance, metal resistivity, and the morphology of the contacts were studied. The results show that samples doped in the range of 10^{18} cm^{-3} had Schottky-like *I–V* characteristics and only samples doped 1.6×10^{19} cm^{-3} exhibited ohmic behavior even before annealing. For the ohmic contacts, increasing annealing temperature causes a decrease in the specific contact resistance ($\rho_{c,Ti/Pd/Ag} \sim 5 \times 10^{-4}$ Ω cm^2). In regard to the metal resistivity, Ti/Pd/Ag metallization presents a very good metal conductivity for samples treated below 500°C ($\rho_{M,Ti/Pd/Ag} \sim 2.3 \times 10^{-6}$ Ω cm); however, for samples treated at 750°C, metal resistivity is strongly degraded due to morphological degradation and contamination in the silver overlayer. As compared to the classic AuGe/Ni/Au metal system, the Ti/Pd/Ag system shows higher metal/semiconductor specific contact resistance and one order of magnitude lower metal resistivity.

Key words: Ohmic contact, *n*-GaAs, high conductivity

INTRODUCTION

The formation of high quality metal/semiconductor contacts has been an open topic in semiconductor technology research for several decades.[1,2] A broad variety of metallization systems on GaAs have been investigated and most of them are designed to improve the low metal–semiconductor specific contact resistance and enhance the contact bondability.[3–6] However, for some devices using GaAs contact layers, such as light emitting diodes (LEDs), lasers or solar cells, low metal resistivity is also very important due to the inherent presence of large current densities in them. Moreover, in the case of LEDs and solar cells, this problem is specially demanding since the front contact has the form of a grid (i.e., does not fully cover the front side) and thus the problem of high current densities is aggravated by a contact with limited area.[7–9] These devices typically use gold in their metal contacts; for example, the AuGe/Ni/Au contact on *n*-GaAs is a classic metallization that has been the dominant scheme in many III–V devices on account of its low contact resistance and good adherence.[10–12] However, despite producing very low metal/semiconductor specific contact resistances ($\sim 10^{-6}$ Ω cm^2), this system is not optimal since: (1)

(Received July 29, 2015; accepted February 24, 2016)

Au has intermetallic reactions with GaAs (i.e., compromising the long term stability of the metal/semiconductor interface); (2) Au is very expensive; and (3) the conductivity of the gold overlayer -i.e., the part of the metal stack intended to provide low metal resistivity- is significantly degraded by the in-diffusion of Ni and Ge from the contact layer and Ga and As from the semiconductor, since Ni does not work as a good barrier layer during the rapid thermal annealing (RTA) process. For these reasons, several other metallization systems have been studied to meet these requirements. For example, one method has targeted the minimization of the crossed-diffusions in the AuGeNi system by optimizing the RTA temperature[13] or introducing a barrier layer to stop it.[14] Another strategy has been based on using totally different metal stacks. In this field, the study of metallizations based on Ti/Pt or Ti/Pd has been intense since both Ti and Pt or Pd work as efficient barrier layers and Ti also promotes the adhesion of the contact to the semiconductor.[15–17] Some other metal systems receiving some attention over the last years include metallizations based on Pd/Ge, which exploit the inward diffusion of Ge and the formation of a highly doped semiconductor and/or barrier height lowering stemming from the formation of a Ge-GaAs heterojunction,[18–21] and some other similar metallization systems such as Pd/Sn, Ge/Cu.[22] In summary, the search of a new metal system providing (1) low metal/semiconductor specific contact resistance ($<10^{-5}$ Ω cm^2); (2) low metal sheet conductivity; (3) high long term stability; (4) good bondability and (5) low cost is still an open field of research.

In the field of silicon solar cells—in particular, in high efficiency or concentrator designs—this problem was solved using the system Ti/Pd/Ag to define front grids on n-Si, with evidence of excellent metal/semiconductor specific contact resistance, good bondability, and demonstrated long-term stability.[23,24] These properties can be cursorily explained as follows: (1) Ti is a refractory metal that while having an firm adhesion to Si, does not show intermetallic reactions (at least for $T < 500$°C), providing excellent stability and total absence of spiking at the metal semiconductor interface; (2) high doping levels in Phosphorus-diffused solar cell emitters and Ti's ability to dissolve the native SiO_2 produce extremely thin Schottky barriers and very low specific contact resistances; (3) Ti/Pd works as a diffusion barrier layer, separating the Si and top Ag layer, and thus avoiding cross contamination; and (4) pure Ag has a large conductivity, ideal to produce contacts with low metal resistivity. In summary, the Ti/Pd/Ag metallization has been reported to work fine on n^+Si.

Moving on to GaAs, Ti has been extensively studied to fabricate highly stable Schottky contacts on moderately doped n-GaAs[25–27] for its ability to produce inert and highly stable interfaces. Figure 1 shows the energy band diagrams of Ti/n-GaAs contacts for various doping levels in the GaAs layer (left $N_D = 1 \times 10^{18}$ cm^{-3}; center $N_D = 3 \times 10^{18}$ cm^{-3}; right $N_D = 1 \times 10^{19}$ cm^{-3}). All the diagrams in this figure have been calculated using Snider's 1-D Poisson solver[28] assuming the Ti/n-GaAs barrier layer to be $\phi_{M\text{-}S} = 0.8$ eV.[26,27] Obviously, the resulting effective barrier thickness ($W_{M\text{-}S}$)—defined here as the depth at which the conduction band energy reaches the Fermi level energy—is the parameter that controls the conduction of charge carriers across this interface by governing their tunneling probability. For moderately doped n-GaAs layers (data not shown), $W_{M\text{-}S}$ can extend over a hundred nm but it also can reach values lower than 300 Å for dopings higher than 1.5×10^{18} cm^{-3}, indicating that (as occurs with n^+Si) heavy doping in the contact layer is an effective way to control the transition from Schottky to ohmic behavior.

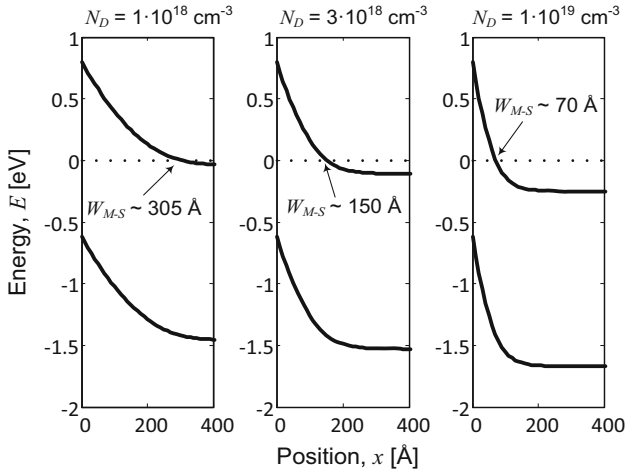

Fig. 1. Energy band diagrams of Ti/n-GaAs contacts for various doping levels in the GaAs layer (left $N_D = 1\times10^{18}$ cm^{-3}; center $N_D = 3\times10^{18}$ cm^{-3}; right $N_D = 1\times10^{19}$ cm^{-3}). The zero energy level is the Fermi energy level. All the diagrams have been calculated assuming the Ti/n-GaAs barrier layer to be $\phi_{M\text{-}S} = 0.8$ eV. The resulting effective barrier thickness ($W_{M\text{-}S}$) for each doping level are also included in the plots.

Therefore, the aforementioned working principles of the Ti/Pd/Ag metal system on n^+Si also hold for n^+GaAs, and therefore this metal system shows some potential for our target application. First, it should be noted that Ti also shows firm adhesion to GaAs and does not react with it at least for $T < 500$°C,[25] providing excellent stability of the metal semiconductor interface. Second, Ti affinity for oxygen also provides an advantage over GaAs, since it can be used to get oxygen during the e-beam evaporation process and to dissolve the native GaAs oxides to produce clean sharp metal–semiconductor interfaces. Third, as shown in Fig. 1, high doping levels in the n-GaAs produce very thin Schottky barriers with potentially low specific contact resistance. In addition, Ti also works as a diffusion

barrier in GaAs,[15–17,25] separating the semiconductor and the top metal layer in charge of providing good sheet conductance; the endurance of this barrier is further enhanced by the presence of a layer of Pd.[17] Finally, pure Ag has a large conductivity, ideal to produce contacts with low metal resistivity.

In fact, pursuing some of these ideas, there are some works in the literature reporting the use of Ti/Pd/Au on p-GaAs,[29] and other Ti-based contacts on GaAs, such as Ti/Pt for p-GaAs[30,31] and Ti/Pt/Au for *n*-GaAs.[15,16] In these systems either gold (and not silver) is used as the conductive layer or Pt (and not Pd) is used as the diffusion barrier layer. Although Pt has been shown to have superior performance than Pd working as a diffusion barrier (because the Pd-Pd bond strength is about one fourth of that of the Pt-Pt bond), the fact is that Pd has demonstrated to be successful under moderate RTA temperatures (<500°C) and is more cost-effective.[29,30]

Despite its potential advantages, a thorough study of Ti/Pd/Ag metallization characteristics on *n*-GaAs is lacking, and would offer a more cost-effective alternative than systems using Pt and Au. Accordingly, in this paper we present an assessment of Ti/Pd/Ag contacts to *n*-GaAs as a function of the *n*-GaAs doping level and contact annealing treatment; analyzing the impact of these variables on the Schottky/Ohmic nature of the contact; its specific contact resistance, and the influence of contact formation on the metal resistivity and morphology (i.e., bondability) of the metallization.

EXPERIMENTAL PROCEDURES

A set of *n*-GaAs layers were grown by metalorganic vapor phase epitaxy (MOVPE) on semi-insulating (100) GaAs wafers with a miscut of 2° towards the nearest (111)A plane. The epilayer thickness was of 400 nm and three different doping concentrations of 1.3×10^{18} cm^{-3}, 3.1×10^{18} cm^{-3}, and 1.6×10^{19} cm^{-3} were fabricated to observe the doping level influence on the contact quality. Such doping levels were chosen to sweep typical contact layer doping levels used in MOVPE. After epitaxial growth, the doping level in the *n*-GaAs layers was confirmed by electrochemical capacitance–voltage profiling using a WEP Control CVP21 tool. Contact areas were defined by using conventional photolithographic techniques. Prior to contact deposition, the substrates were cleaned using H_2SO_4:H_2O_2:H_2O (2:1:50) and HCl:H_2O (1:1) to remove the native oxide layer, and a completely hydrophobic surface was obtained; deionized water rinsing and blown dry with nitrogen followed. Ti/Pd/Ag metal stacks of 50 nm/50 nm/1000 nm were deposited in a multi-pocket electron beam evaporator at a base vacuum of 1×10^{-6} mbar. Immediately after evaporation, the patterns suffered a lift-off process to take away the metal from unwanted areas. The samples were separately annealed by RTA in forming gas (H_2:N_2, 1:9) at different temperatures (300–750°C) and times (20–180 s). In order to compare the quality of the metallization obtained, samples with the classic contact structure AuGe/Ni/Au (200 nm/60 nm/500 nm) were also fabricated on the highest doped layer (1.6×10^{19} cm^{-3}) and RTA processing at 375°C for 180 s. For the electrical characterization, the transmission line model (TLM)[32] was used to measure specific contact resistance and the Van der Pauw method[33] was used to measure the metal layer sheet resistance, and the metal resistivity was calculated by sheet resistance times the measured thickness of the metal layer. To insulate both the TLM and Van der Pauw patterns, a mesa etching was done with NH_4OH:H_2O_2:H_2O (2:1:10). The electrical characterization was carried out using the 4-wires method by sweeping current and measuring voltage (in order to obtain better measurements in the low current range, the samples doped 1.3×10^{18} cm^{-3} were measured by sweeping voltage and measuring current) using a Keithley 2062 programmable power supply. A profilometer KLA-Tencor Alpha-Step D-120 Stylus Profiler was used to measure the surface roughness.

RESULTS AND DISCUSSION

In the first set of the experiments, Ti/Pd/Ag layers (50 nm/50 nm/1000 nm) were deposited on three *n*-GaAs layers with different doping levels (1.3×10^{18} cm^{-3}, 3.1×10^{18} cm^{-3}, and 1.6×10^{19} cm^{-3}) and subsequently annealed by RTA at 400°C for 100 s. Figure 2 shows, for each sample, representative *I-V* curves taken between two adjacent TLM contacts, which were 100 μm apart.

Figure 2 is evidence that, when the doping level is not high enough, Schottky contacts are obtained. Nevertheless, for the sample doped 1.6×10^{19} cm^{-3}, the contact is ohmic and shows little influence of the RTA process (curves for annealed and non-annealed

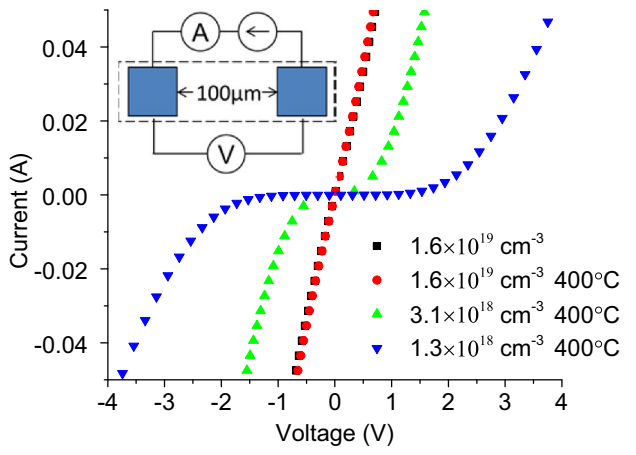

Fig. 2. *I–V* curve of Ti/Pd/Ag contact resistance as a function of *n*-GaAs doping. Pad separation is 100 μm.

samples virtually overlap in Fig. 2). The specific contact resistance and metal resistivity of these samples are included in Table I. As anticipated by Fig. 2, the specific contact resistance ρ_c experiences only small changes before and after RTA, going from $\rho_c = 1.9 \times 10^{-3}\ \Omega\ cm^2$ to $\rho_c = 1.5 \times 10^{-3}\ \Omega\ cm^2$. However, despite being ohmic, these values of ρ_c are still quite high, as compared to the reference AuGe/Ni/Au contact (last row in Table I). On the contrary, the values of metal resistivity ρ_M are significantly better and quite homogeneous for all samples in Fig. 2. All values of ρ_M are around $2.4 \times 10^{-6}\ \Omega$ cm, which is about one magnitude lower than the metal resistivity of the AuGe/Ni/Au reference contact. Notably, this metal resistivity range is reasonably close to its tabulated value for pure bulk material ($1.6 \times 10^{-6}\ \Omega$ cm). Given the fact that even small impurity concentrations tend to affect the conductivity of thin films, it seems plausible that the Ag layer is not contaminated by GaAs, supporting the idea that TiPd works fine as a barrier layer, hindering the diffusion of Ga and As atoms into the Ag layer. Of course this result is not an unequivocal proof for lack of significant diffusion, though it is certainly in line with the results with Ti/Pd/Au reported by Chor et al.[29] and Jones et al.,[30] where no significant contamination of the Au layer could be measured for RTA processing temperatures of 500°C or less. On the contrary, the metal resistivity of the AuGe/Ni/Au system is one order of magnitude lower than that of pure bulk gold. This seems to be an indirect evidence of Ni not being as an effective diffusion barrier and thus gold overlayer conductivity being degraded by Ga and As, Ge, and Ni contamination.

To assess the impact of annealing conditions on the Ti/Pd/Ag contact quality, different RTA processes have been carried out. Figure 3a shows the results for the contacts made on GaAs doped $1.3 \times 10^{18}\ cm^{-3}$. In all cases, Schottky-like behavior is observed. For increasing temperatures a slight decrease in the turn-on voltage (i.e., on the barrier height) is observed. At this point, it seemed plausible that further increasing the annealing temperature would eventually make the contact ohmic.

Therefore, the experiment was repeated and higher temperatures were explored for the RTA. In order to further facilitate the formation of ohmic contacts (i.e., in order to increase tunneling probability), highly doped samples ($N_D = 3.1 \times 10^{18}\ cm^{-3}$) were used in this new set of experiments. The result of this experiment can be seen in Fig. 3b. As shown in this figure, when the annealing temperature is raised to 750°C, which is the optimum temperature for a Ti contact on degenerated doped n-GaAs as reported by Zhou et al.[15] the contact becomes ohmic and $\rho_c = 9.2 \times 10^{-4}\ \Omega\ cm^2$. However, for lower temperatures (400°C and 500°C), Schottky contacts are obtained as displayed in Fig. 3b.

Finally, Fig. 3c summarizes the same set of experiments for the sample doped $1.6 \times 10^{19}\ cm^{-3}$. As shown in Fig. 3c and Table I, an increase in annealing temperature mildly decreases ρ_c. After annealing at 750°C, a minimum ρ_c value is reached of $1.3 \times 10^{-4}\ \Omega\ cm^2$, which is similar to the results obtained with Ti/Pt/Au on n-GaAs($\sim 1.0 \times 10^{-4}\ \Omega\ cm^2$);[15,16] still far from the values of the reference AuGe/Ni/Au contact ($\rho_c = 2.9 \times 10^{-6}\ \Omega\ cm^2$) and metallization systems based on Pd/Ge on n-GaAs($\sim 3.0 \times 10^{-7}$).[19,21,34] Obviously, the

Table I. Comparison of contact properties of Ti/Pd/Ag on *n*-tpye GaAs with different doping and annealing conditions

System	Doping concentration N_D (cm^{-3})	RTA	Specific contact resistance ρ_c ($\Omega\ cm^2$)	Metal resistivity ρ_M (Ω cm)
Ti/Pd/Ag (50 nm/50 nm/1000 nm)	1.3×10^{18}	375°C 180 s	–	2.36×10^{-6}
		400°C 100 s	–	2.38×10^{-6}
		430°C 100 s	–	2.47×10^{-6}
		460°C 100 s	–	2.49×10^{-6}
Ti/Pd/Ag (50 nm/50 nm/1000 nm)	3.1×10^{18}	–	–	2.02×10^{-6}
		400°C 100 s	–	2.48×10^{-6}
		500°C 100 s	–	2.14×10^{-6}
		750°C 30 s	9.2×10^{-4}	7.19×10^{-5}
Ti/Pd/Ag (50 nm/50 nm/1000 nm)	1.6×10^{19}	–	1.9×10^{-3}	1.98×10^{-6}
		400°C 100 s	1.5×10^{-3}	2.23×10^{-6}
		500°C 100 s	4.9×10^{-4}	2.23×10^{-6}
		750°C 30 s	1.3×10^{-4}	9.31×10^{-5}
AuGe/Ni/Au (200 nm/60 nm/500 nm)	1.6×10^{19}	375°C 180 s	2.9×10^{-6}	2.22×10^{-5}

The time included in the third column is the so-called *soaking time* for the RTA process (i.e., the time for which the temperature remains constant, not including ramp-up and ramp-down times). The results of the classic AuGe/Ni/Au metallization have been included for reference in the last row.

Journal : 11664_JEM Dispatch : 2-3-2016 Pages : 7
Article No.: 4432 ☐ LE ☑ CP ☐ TYPESET ☑ DISK

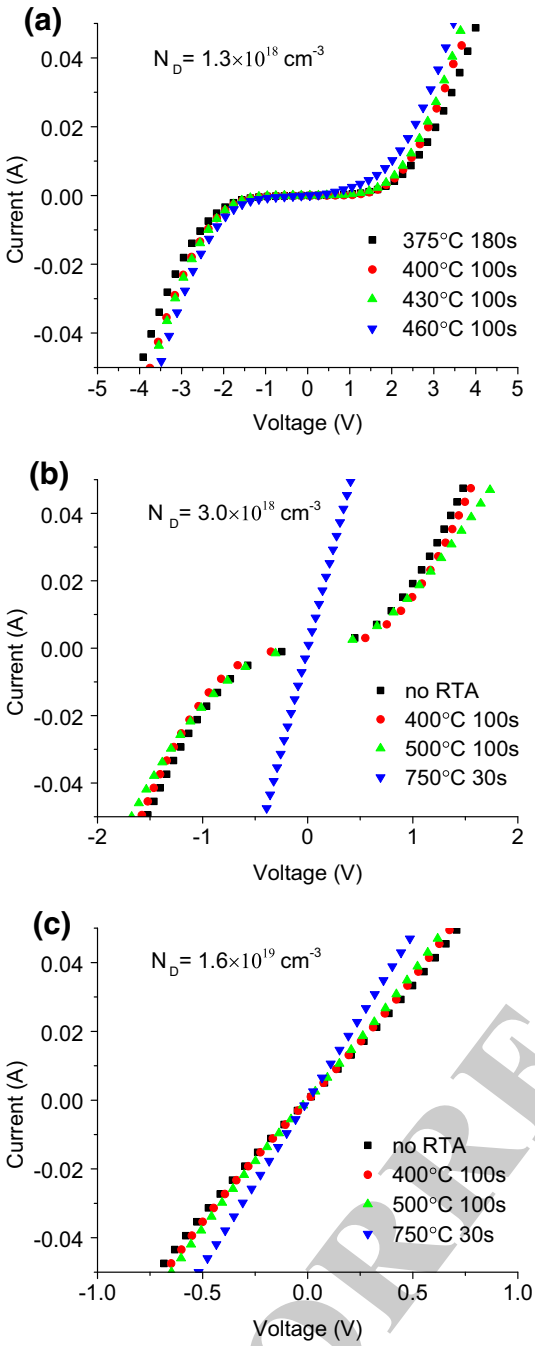

Fig. 3. *I–V* curves of Ti/Pd/Ag contact resistance as a function of annealing temperature and doping level. The *n*-GaAs layer doping concentration is: (a) $N_D = 1.3 \times 10^{18}$ cm^{-3}; (b) $N_D = 3.1 \times 10^{18}$ cm^{-3}; (c) and $N_D = 1.6 \times 10^{19}$ cm^{-3}. Pad separation is 100 μm in all cases. Please note the different voltage scale in the three figures.

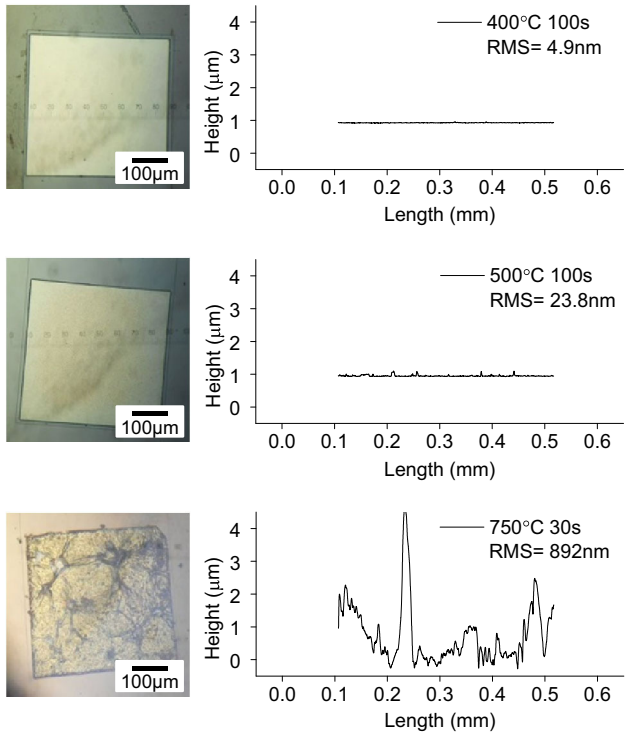

Fig. 4. Surface roughness of Ti/Pd/Ag contacts deposited on 3.1×10^{18} cm^{-3} doped *n*-type GaAs with different annealing conditions.

high ρ_c limitation places restrictions on the use of this metallization system; however, it could be acceptable in some cases. For example, according to the calculation reported by Cotal et al.[16] it could be used with low or medium concentrator photovoltaic (CPV) solar cells operating below 500 suns. Nevertheless, given the fact that many CPV manufacturers are moving their designs to ultra-high concentration levels (above 1000 suns), ρ_c needs to be improved to values below 1×10^{-5} Ω cm^2.

Table I also summarizes the results of metal resistivity of the experiments in Fig. 3a–c. A first fact observable in this table is that annealing temperatures lower than 500°C seem not to affect significantly the metal resistivity of the layer. The metal resistivity barely increases after annealing below 500°C. Furthermore, the average metal resistivity of all these experiments from 375°C to 500°C is 2.4×10^{-6} Ω cm with a standard deviation of around 6%, which is in agreement with the uncertainty expected in the deposited thickness in our e-gun evaporator. In other words, if there is a change in metal resistivity associated with annealing the samples for temperatures from 375°C to 500°C, it is not observable due to the uncertainty in the deposited thickness. However, this situation changes for the samples processed at 750°C. In such a case, the metal resistivity is highly degraded, increasing by more than a factor of 30.

In order to gain insight into these changes of the metal resistivity, the surface roughness of samples annealed at different temperatures was measured using a profilometer, as shown in Fig. 4. This figure shows that sample roughness increases with annealing temperature and surface roughness (RMS) increases from 4.9 nm to 892 nm, reaching

a deleterious morphology for samples annealed at 750°C. In addition, the color of the metallization changed from silver to bronze-green after annealing at 750°C, evidencing some chemical (intermetallic) reactions between the components of the metal system possibly as a result of the blurring of the Ti/Pd barrier layer.[35,36] In summary, morphology degradation together with the degradation of Ag conductivity as a result of contamination could explain the degradation measured and calculated in the metal resistivity.

SUMMARY AND CONCLUSIONS

Ti/Pd/Ag metallizations on *n*-GaAs have been studied in the quest for a metal system that can provide (1) low metal/semiconductor specific contact resistance; (2) low metal conductivity; (3) high long-term stability; (4) good bondability; and (5) low cost as compared to traditional gold-based systems.

In terms of contact resistance, we found that samples doped in the range of 10^{18} cm^{-3} had Schottky-like *I–V* characteristics, and only samples doped in the range of 10^{19} $cm^{-3,}$ exhibited ohmic behavior even before RTA. For the Schottky contacts, we observed a decrease in the Schottky barrier with increasing RTA temperature. For the ohmic contacts, non-annealed samples had a metal/semiconductor specific contact resistance of $\rho_c \sim 2\times10^{-3}$ Ω cm^2, whilst in annealed samples ρ_c decreased with RTA temperatures down to $\rho_c \sim 5\times10^{-4}$ Ω cm^2 for samples treated at 500°C. In samples annealed at 750°C, ρ_c went further down to $\rho_c \sim 1\times10^{-4}$ Ω cm^2 at the expense of a total degradation of the morphology and evidence of intermetallic reactions in the silver overlayer.

Regarding metal resistivity, we found that Ti/Pd/Ag contacts on *n*-tpye GaAs present a very good metal resistivity as far as RTA temperatures are kept below 500°C. In fact, our measurements show that the conductivity of the silver overlayer virtually equals that of pure bulk Ag. This fact would be in agreement with Ag being free of contamination and the Ti/Pd bilayer acting as an efficient diffusion barrier for Ga and As for temperatures below 500°C as observed in other works. Above this temperature, morphological degradation and contamination in the silver overlayer strongly degrade metal resistivity. These results have been compared to the classic AuGe/Ni/Au metal system for which metal/semiconductor specific contact resistance is two orders of magnitude lower ($\rho_{c,AuGe/Ni/Au} \sim 3\times10^{-6}$ Ω cm^2 and $\rho_{c,Ti/Pd/Ag} \sim 5\times10^{-4}$ Ω cm^2) while the metal resistivity is a factor of 10 larger ($\rho_{M,AuGe/Ni/Au} \sim 2.4\times10^{-5}$ Ω cm, as compared $\rho_{M,Ti/Pd/Ag} \sim 2.3\times10^{-6}$ Ω cm).

In conclusion, the good metal resistivity of the Ti/Pd/Ag system shows promise to develop ohmic contacts to electronic devices that handle large current densities. The lowest values reached for the metal/semiconductor specific contact resistance are still far from the records reported in the literature, though would be enough to be used in low or medium concentration solar cells (<500 suns). Future work will be dedicated to enhance the metal–semiconductor specific contact resistance, which could be accomplished by introducing other metal layers between Ti and GaAs.

ACKNOWLEDGEMENTS

Mr. Huo Pengyun acknowledges financial support of the China Scholarship Council for his Ph.D. This work was supported by the Spanish Ministerio de Economía y Competitividad through Project with reference TEC2012-37286. We also acknowledge Fundación Iberdrola for their financial support within the Program "Ayudas a la Investigación en Energía y Medioambiente".

REFERENCES

1. L.J. Brillson, *Contacts to Semiconductors: Fundamentals and Technology* (Park Ridge, New Jersey: Noyes, 1993), pp. 1–3.
2. D.K. Schroder and D.L. Meier, *IEEE Trans. Electron. Dev.* 31, 637 (1984).
3. V.L. Rideout, *Solid State Electron.* 18, 541 (1975).
4. A. Piotrowska, A. Guivarc'h, and G. Pelous, *Solid State Electron.* 26, 179 (1983).
5. A. Piotrowska, *Acta Phys. Pol. A* 84, 491 (1993).
6. A.G. Baca, F. Ren, J.C. Zolper, R.D. Briggs, and S.J. Pearton, *Thin Solid Films* 308–309, 599 (1997).
7. D.L. Meier and D.K. Schroder, *IEEE Trans. Electron. Dev.* 31, 647 (1984).
8. A.R. Burgers, *Prog. Photovolt.* 7, 457 (1999).
9. M.M. Shabana, M.B. Saleh, and M.M. Soliman, *Solar Cells* 26, 177 (1989).
10. N. Braslau, J.B. Gunn, and J.L. Staples, *Solid State Electron.* 10, 381 (1967).
11. T.S. Kuan, P.E. Batson, T.N. Jackson, H. Rupprecht, and E.L. Wilkie, *J. Appl. Phys.* 54, 6952 (1983).
12. Y.C. Shih, M. Murakami, E.L. Wilkie, and A.C. Callegari, *J. Appl. Phys.* 62, 582 (1987).
13. A.G. Baca and C.I.H. Ashby, *Fabrication of GaAs Devices* (London: Institution of Electrical Engineers, 2005), p. 196.
14. Y. Wang, D. Liu, G. Feng, Z. Ye, Z. Gao, and X. Wang, *J. Semicond.* 36, 036002 (2015).
15. J. Zhou, G. Xia, B. Li, and W. Liu, *Appl. Phys. A* 76, 939 (2003).
16. H. Cotal, C. Fetzer, J. Boisvert, G. Kinsey, R. King, P. Hebert, H. Yoon, and N. Karam, *Energy. Environ. Sci.* 2, 174 (2009).
17. W.K. Chong, E.F. Chor, C.H. Heng, and S.J. Chua, *Inst. Phys. Conf. Ser.* 156, 171 (1998).
18. K.C. Sahoo, C.W. Chang, Y.Y. Wong, T.L. Hsieh, E.Y. Chang, and C.T. Lee, *J. Electron. Mater.* 37, 901 (2008).
19. D.G. Ivey, S. Eicher, S. Wingar, and T. Lester, *J. Mater. Sci.* 8, 63 (1997).
20. C.-H. Hsu, H.-J. Chang, H.-W. Yu, H.-Q. Nguyen, J.-S. Ma, E.Y. Chang, and I.E.E.E. Int, *Conf. Semicond. Electron.* (2014). doi:10.1109/SMELEC.2014.6920866.
21. C. Gutsche, A. Lysov, I. Regolin, A. Brodt, L. Liborius, J. Frohleiks, W. Prost, and F.-J. Tegude, *J. Appl. Phys.* 110, 014305 (2011).
22. T.V. Blank and Y.A. Gol'dberg, *Semiconductors* 41, 1263 (2007).
23. H. Fischer and R. Gereth, *IEEE Trans. Electron. Dev.* 18, 459 (1971).
24. X. Loozen, J.B. Larsen, F. Dross, M. Aleman, T. Bearda, B.J. O'Sullivan, I. Gordon, and J. Poortmans, *Energy Procedia* 21, 75 (2011).
25. A.K. Sinha, T.E. Smith, M.H. Read, and J.M. Poate, *Solid State Electron.* 19, 489 (1976).

26. B.K. Sehgal, B. Bhattacharya, S. Vinayak, and R. Gulati, *Thin Solid Films* 330, 146 (1998).
27. T. Göksu, N. Yıldırım, H. Korkut, A.F. Özdemir, A. Turut, and A. Kökçe, *Microelectron. Eng.* 87, 1781 (2010).
28. I.-H. Tan, G.L. Snider, L.D. Chang, and E.L. Hu, *J. Appl. Phys.* 68, 4071 (1990).
29. E.F. Chor, D. Zhang, H. Gong, W.K. Chong, and S.Y. Ong, *J. Appl. Phys.* 87, 2437 (2000).
30. K.A. Jones, M.W. Cole, W.Y. Han, D.W. Eckart, K.P. Hilton, M.A. Crouch, and B.H. Hughes, *J. Appl. Phys.* 82, 1723 (1997).
31. A. Katz, C.R. Abernathy, and S.J. Pearton, *Appl. Phys. Lett.* 56, 1028 (1990).
32. G.K. Reeves and H.B. Harrison, *IEEE Electr. Device Lett.* 3, 111 (1982).
33. L.J. van der Pauw, *Philips Res. Rep.* 13, 1 (1958).
34. J.-L. Lee, Y.-T. Kim, J.-W. Oh, and B.-T. Lee, *Jpn. J. Appl. Phys.* 40, 1188 (2001).
35. O. Wada, S. Yanagisawa, and H. Takanashi, *Appl. Phys. Lett.* 29, 263 (1976).
36. M. Kniffin and C.R. Helms, *J. Vac. Sci. Technol. A* 5, 1511 (1987).

Journal : 11664_JEM | Dispatch : 2-3-2016 | Pages : 7
Article No.: 4432 | ☐ LE ☑ CP | ☐ TYPESET ☑ DISK